



## OPEN

CO<sub>2</sub>-based in-line phase contrast imaging of small intestine in miceRongbiao Tang<sup>1</sup>, Wei-Xia Li<sup>1</sup>, Wei Huang<sup>1</sup>, Fuhua Yan<sup>1</sup>, Wei-Min Chai<sup>1</sup>, Guo-Yuan Yang<sup>2</sup> & Ke-Min Chen<sup>1</sup>

## SUBJECT AREAS:

PRE-CLINICAL STUDIES

OPTICAL IMAGING

BIOLOGICAL PHYSICS

PHASE-CONTRAST MICROSCOPY

<sup>1</sup>Department of Radiology, Rui Jin Hospital, Shanghai Jiao Tong University School of Medicine, Shanghai 200025, PRC,<sup>2</sup>Neuroscience and Neuroengineering Center, Med-X Research Institute, Shanghai Jiao Tong University, Shanghai 200030, PRC.Received  
15 May 2013Accepted  
11 July 2013Published  
30 July 2013

The objective of this study was to explore the potential of CO<sub>2</sub> single contrast in-line phase contrast imaging (PCI) for pre-clinical small intestine investigation. The absorption and phase contrast images of CO<sub>2</sub> gas production were attained and compared. A further increase in image contrast was observed in PCI. Compared with CO<sub>2</sub>-based absorption contrast imaging (ACI), CO<sub>2</sub>-based PCI significantly enhanced the detection of mucosal microstructures, such as pits and folds. The CO<sub>2</sub>-based PCI could provide sufficient image contrast for clearly showing the intestinal mucosa in living mice without using barium. We concluded that CO<sub>2</sub>-based PCI might be a novel and promising imaging method for future studies of gastrointestinal disorders.

Correspondence and requests for materials should be addressed to

R.T.

(tangme8688258@sina.com) or K.M.C.

(keminchenrj1@yahoo.com.cn)

For a long time, the small intestine has been the most difficult segment of the gastrointestinal tract to examine<sup>1–3</sup>. Endoscopy is a valuable tool in the evaluation of small intestinal disease, but the procedure usually produces discomfort. Moreover, most part of the small intestine is inaccessible to endoscopy<sup>4</sup>. Capsule endoscopy is a good way to noninvasively visualize the entire small bowel mucosa<sup>2,5</sup>. However, the lesions are usually detected by accident, so they may be missed if the capsule endoscopy does not take an image as it moves through an area of disease<sup>1</sup>. CO<sub>2</sub>-barium double contrast gastrointestinalgraphy is a common clinical tool to assess gastrointestinal conditions. Before the examination, some aerogenic powders are taken orally by the patient. Aerogenic powders mainly contain a mixture of citric acid and NaHCO<sub>3</sub>. Reactions between the dry powders won't take place until they encounter water. The chemical reaction equation is as follows: citric acid + NaHCO<sub>3</sub> + water → sodium citrate + CO<sub>2</sub> + water. The gastrointestinal tract will be expanded by the produced CO<sub>2</sub> gas. The CO<sub>2</sub>-barium double contrast x-ray imaging can not only provide optimal visualization of mucosal abnormalities, but also evaluate the intestinal peristaltic function. However, barium will be forbidden if a patient is suspected of gastrointestinal perforation or complete obstruction. In this case, CO<sub>2</sub> single contrast x-ray imaging seems to be a safe method to be chosen. Still, conventional radiography always provides poor image contrast for soft tissues which have low differential absorption of x-rays. Because the gastrointestinal tract is the soft tissue tube, and the density difference between the mucosa and CO<sub>2</sub> is small, the mucosal structures were hardly detected by CO<sub>2</sub> single contrast gastrointestinalgraphy (Fig. 1).

It has been demonstrated that synchrotron radiation phase contrast imaging (SR-PCI) has outstanding potential for medical applications<sup>6,7</sup>. By utilizing the phase shift, SR-PCI can offer superb image contrast for soft tissues<sup>8–12</sup>. Because the gas has a different refractive index from the surrounding soft tissues, the gas-tissue interfaces create significant phase shifts to make the boundaries highly visible in PCI<sup>8,13</sup>. By means of the detection of the phase shift generated by intestinal mucosa and CO<sub>2</sub>, PCI may enable to provide clear visualization of CO<sub>2</sub>-filled mucosa of small intestine without using barium.

In this study, we first report the pre-clinical applications of CO<sub>2</sub>-based in-line PCI for small intestine research. CO<sub>2</sub>-based SR absorption contrast imaging (ACI) and PCI were performed and compared. CO<sub>2</sub> gas produced by aerogenic powders was imaged real-timely by PCI. Additionally, the potential of CO<sub>2</sub> single contrast PCI for showing small intestinal mucosal microstructures in living mice was investigated.

## Results

**Comparison between CO<sub>2</sub> gas-based ACI and PCI.** No CO<sub>2</sub> bubbles could be obtained before physiological saline injection (Fig. 2c,g). After physiological saline was injected, aerogenic powders reacted with water to produce CO<sub>2</sub> gas. However, the difference in the x-ray absorption of the CO<sub>2</sub> gas and physiological saline is small, so the CO<sub>2</sub> bubbles could hardly shown in ACI (Fig. 2e). Since CO<sub>2</sub> has a different refractive index from

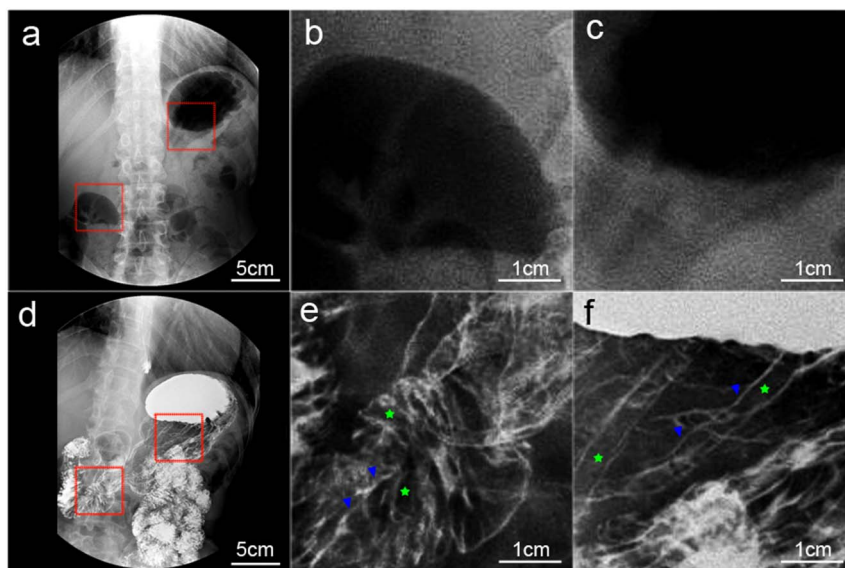


**Figure 1** | The gastrointestinalgraphy of a 50-year-old female patient with abdominal discomfort after administration of CO<sub>2</sub> gas only (a), or CO<sub>2</sub> gas and barium (d). (b–c) and (e–f) are magnified images of the red boxed regions in (a) and (d), respectively. Note that CO<sub>2</sub>-barium double contrast gastrointestinalgraphy (e–f) provided clear visualization of mucosal folds (asterisks) and intermucosal grooves (arrowheads), which were hardly shown on CO<sub>2</sub> single contrast gastrointestinalgraphy (b–c).

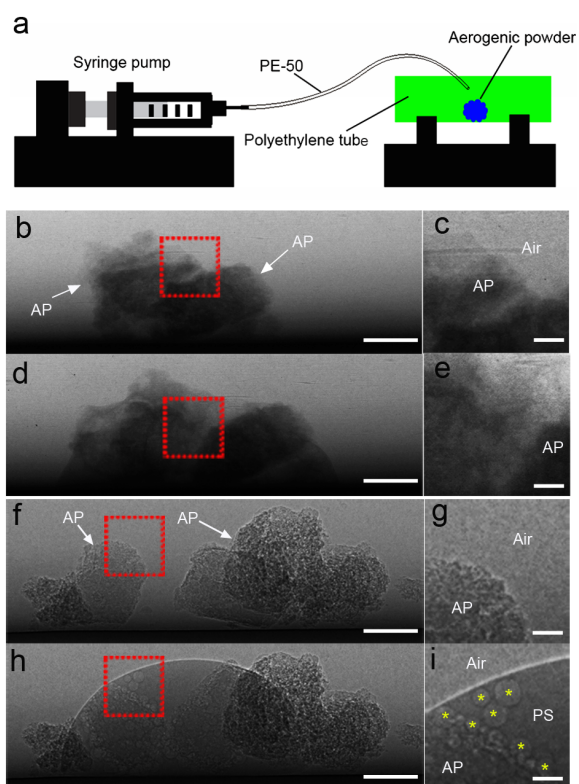


**Figure 2** | ACI and PCI of CO<sub>2</sub> gas production. (a) The experimental setup for generating CO<sub>2</sub> gas. Aerogenic powders were placed in a polyethylene tube which was perpendicular to the x-ray beam. Physiological saline was injected to the aerogenic powders through a PE-50 tube connected to a syringe pump. ACI (b,d) and PCI (f,h) of aerogenic powders before (b,f) and after (d,h) the physiological saline injection. (c), (e), (g) and (i) are magnified images of the red boxed regions in (b), (d), (f) and (h), respectively. Note that the production of CO<sub>2</sub> bubbles could be clearly displayed in phase contrast image (i), but not in absorption contrast image (e). The pixel size was 9 μm × 9 μm; the exposure time was 3 ms. AP indicates aerogenic powders; PS indicates physiological saline. Asterisks indicate CO<sub>2</sub> bubbles. Scale bars: 1 mm (b,d,f,h) and 200 μm (c,e,g,i).

physiological saline, the gas–physiological saline interfaces created significant phase shifts to make the boundaries extremely visible in PCI (Fig. 2i).

**Real-time PCI of CO<sub>2</sub> gas production.** The characteristic of high-temporal resolution for PCI contributes to clearly capturing the CO<sub>2</sub> bubbles production process real-timely. CO<sub>2</sub> gas was clearly shown to be continuously produced, meanwhile, the aerogenic powders gradually dissolved in the physiological saline (Fig. 3, Supplementary movie 1).

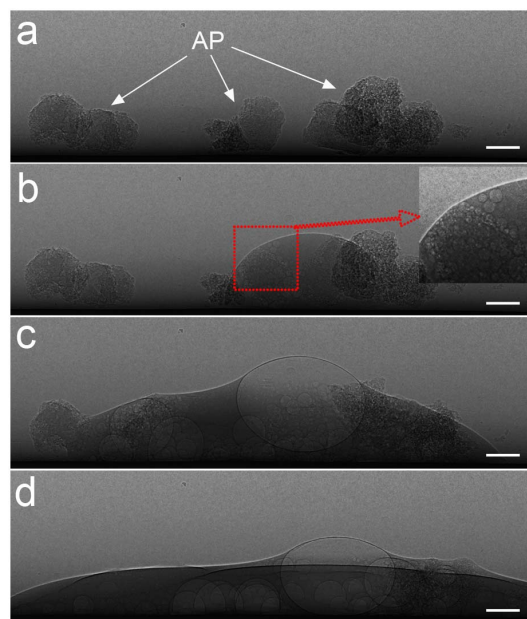


**Figure 3** | Representative, sequential PCI of CO<sub>2</sub> gas production and aerogenic powders solution. CO<sub>2</sub> gas was continuously produced, and the aerogenic powders gradually dissolved in the physiological saline. Images were obtained after the physiological saline injection at 0 s (a), 1 s (b), 30 s (c), and 4 min (d), respectively. The pixel size was 9 μm × 9 μm; the exposure time was 3 ms. AP indicates aerogenic powders. Scale bars: 1 mm.

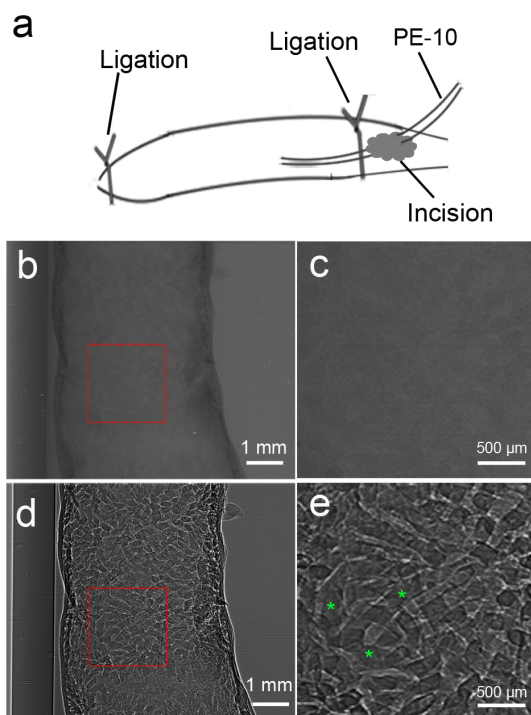


**Figure 4** | *Ex vivo* SR images of the same mouse duodenum with two sample-to-detector distances of 1 cm (b) and 60 cm (d). (a) Schematic of the CO<sub>2</sub> single contrast preparation. (c) and (e) are magnified images of the region in a red box in (b) and (d), respectively. Note that duodenal mucosal microstructures could be more visibly revealed on phase contrast image (e) than on absorption contrast image (c). The pixel size was 3.7 μm × 3.7 μm. The exposure time was 1 s. Asterisks indicate mucosal folds.

**ACI and PCI of small intestine *ex vivo* and *in vivo*.** Because the difference between the absorption coefficients of intestinal mucosa and CO<sub>2</sub> was small, no evident contrast could be detected by ACI (Fig. 4c, 5b). In comparison, PCI exploited the differences in the refractive index and enabled clear visualization of the intestinal microstructures (Fig. 4e, 5d). The CO<sub>2</sub>-based PCI could provide adequate image contrast for clearly showing the intestinal mucosa in living mice without using barium.

## Discussion

Conventional absorption imaging principally employs the absorption characteristics of x-rays, and discriminates different tissues

through the linear attenuation coefficient ( $\mu$ ), which is proportional to the density of the tissue<sup>14</sup>. By taking barium orally, the surface of the gastrointestinal mucosa will be coated with this strong x-ray absorption material. The image contrast can be highly increased to indirectly depict the mucosa. However, barium will be forbidden if bowel perforation or complete obstruction is suspected. Here, we introduce a pre-clinical imaging method to show the mouse mucosal microstructures without using barium. The characteristic of high temporal resolution for PCI is quite suitable for real-time imaging and evaluating the intestinal peristaltic function. Also, PCI can offer high spatial resolution to clearly show several ten microns mouse mucosal folds or pits. Besides high resolution, high sensitivity for soft tissues is another important advantage for PCI. Compared with ACI, PCI can highly enhance image contrast between CO<sub>2</sub> gas and water, indicating a good application of CO<sub>2</sub> as phase contrast agent. CO<sub>2</sub>-based PCI utilizes the phase shifts created by the CO<sub>2</sub>-mucosa interfaces and makes the borders highly detectable. Therefore, the microstructures of the mucosa can be directly and noticeably depicted without using barium.

In summary, PCI is characterized by high spatial-temporal resolution, greatly enhanced contrast, and good soft tissue discrimination. Compared with ACI, PCI is capable of creating notable visibility of CO<sub>2</sub>-filled intestinal mucosa. The CO<sub>2</sub>-PCI technique has great potential for showing small intestinal mucosal microstructure in living mice. It may become a novel *in vivo* imaging tool for future studies of gastrointestinal disorders.

## Methods

**Patient.** A 50-year-old female patient with abdominal discomfort was enrolled for gastrointestinalgraphy with CO<sub>2</sub> single contrast and CO<sub>2</sub>-barium double contrast. Informed consent was obtained from the patient before the examinations. The Ethics Committee for Clinical Research at Shanghai Jiao Tong University, China approved the study protocol.

**SR parameters.** Images were captured at the BL13W1 beamline in Shanghai Synchrotron Radiation Facility (SSRF, China). X-rays were produced from a 3.5 GeV electron storage ring, and were monochromatized using a double-crystal monochromator with Si(111) and Si(311) crystals. The beamline covered an energy range of 8 to 72.5 keV. The energy resolution ( $\Delta E/E$ ) was less than  $5 \times 10^{-3}$ . The transmitted x-rays were captured by a 100-μm thick CdWO<sub>4</sub> cleaved single-crystal scintillator and converted to a visible image. Samples were placed on 34 m downstream of the synchrotron source. The distance between the sample stage and the detector had a changeable range of 8 m (Fig. 6).

**ACI and PCI of CO<sub>2</sub> gas production.** Aerogenic powders (East Wind Chemicals, China) were placed in a polyethylene tube which was perpendicular to the x-ray beam (Fig. 2a). 100 μl physiological saline was injected to the aerogenic powders through a PE-50 tube connected to a computer-controlled syringe pump. ACI and PCI of CO<sub>2</sub> gas production were performed at the energy of 19 keV with two different sample-to-detector distances ( $d = 1$  and 60 cm, respectively). Images were consecutively captured by a CCD camera (Photonic Science, Britain) with the resolution of ~9 μm.

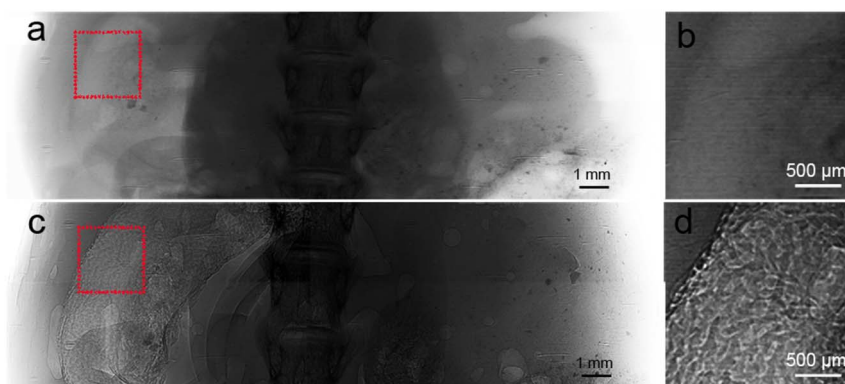


**Figure 5** | *In vivo* SR images of the same mouse duodenum with two sample-to-detector distances of 1 cm (a) and 60 cm (c). (b) and (d) are magnified images of the region in a red box in (a) and (c), respectively. Note that duodenal mucosal microstructures could be more visibly revealed on phase contrast image (d) than on absorption contrast image (b). The pixel size was 9 μm × 9 μm. The exposure time was 5 ms.





## Beamline BL13W1

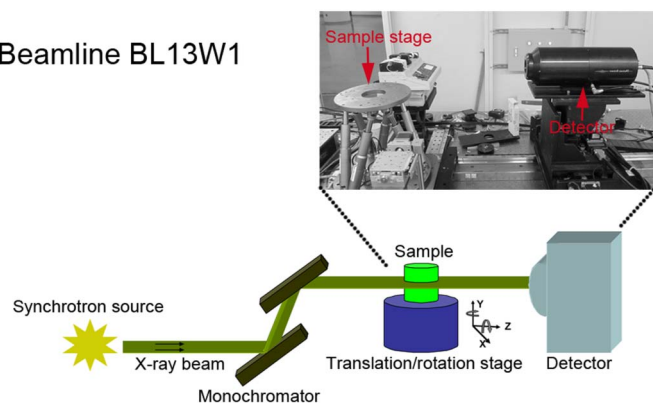


**Figure 6 | Schematic diagram of the in-line PCI set-up at BL13W1 in SSRF.** The distance between the radiation source and the sample stage is 34 m. The inset picture shows that the distance between the sample stage and the detector can be changed from 0 to 8 m by moving the detector on the rail.

**Animals.** All experiments were performed in accordance with guidelines for the care and use of laboratory animals of Shanghai Jiao Tong University. BALB/c mice were purchased from the Animal Center, CAS, Shanghai, China. Animals were housed in a temperature-controlled room with a 12-h light/dark cycle and acclimatized for at least 7 days before use. Prior to imaging, food was withheld overnight with free access to water. Mice were anesthetized using an intraperitoneal injection of ketamine (100 mg kg<sup>-1</sup>) and xylazine (10 mg kg<sup>-1</sup>).

**PCI of CO<sub>2</sub> single contrast preparation.** For imaging small intestine with CO<sub>2</sub> single contrast, duodenum was chosen and gently exteriorized by a mid-line upper abdominal incision after anesthesia. An incision was made on the wall of proximal duodenum. The distal small intestine was ligated at 5 cm from the incision. The intestinal mucosa was fully dried with cotton. Subsequently, 200 µl CO<sub>2</sub> gas was injected to inflate the duodenum by a PE-10 tube through the incision. Then the proximal duodenum near the incision was ligated to prevent CO<sub>2</sub> gas leaking from the incision. The distance between two ligations was 2 cm. For *in vivo* imaging, mice were positioned to set the abdominal cavity perpendicular to the x-ray beam, and then they were imaged by the 9-µm CCD camera. For *ex vivo* imaging, the CO<sub>2</sub> gas-filled duodenum was harvested and imaged using a CCD camera (Photonic Science, Britain) with the resolution of ~3.7 µm. Schematic of the duodenum preparation was shown in Fig 4a. ACI and PCI were performed at the energy level of 19 keV, with the sample-to-detector distance of 1 cm and 60 cm, respectively.

1. Federle, M. P. CT of the small intestine: Enterography and angiography. *Applied Radiology* **36**, 55 (2007).
2. Hara, A. K., Leighton, J. A., Sharma, V. K., Heigh, R. I. & Fleischer, D. E. Imaging of small bowel disease: comparison of capsule endoscopy, standard endoscopy, barium examination, and CT1. *Radiographics* **25**, 697–711 (2005).
3. Zhang, L.-H. *et al.* Multi-detector CT enterography with iso-osmotic mannitol as oral contrast for detecting small bowel disease. *World J Gastroenterol* **11**, 2324–2329 (2005).

4. Sunada, K. *et al.* Clinical outcomes of enteroscopy using the double-balloon method for strictures of the small intestine. *World J Gastroenterol* **11**, 1087–1089 (2005).
5. Ali, A., Santisi, J. M. & Vargo, J. Video capsule endoscopy: a voyage beyond the end of the scope. *Cleveland Clinic journal of medicine* **71**, 415–425 (2004).
6. Lewis, R. Medical phase contrast x-ray imaging: current status and future prospects. *Physics in medicine and biology* **49**, 3573 (2004).
7. Zhou, S.-A. & Brahme, A. Development of phase-contrast X-ray imaging techniques and potential medical applications. *Physica medica: PM: an international journal devoted to the applications of physics to medicine and biology: official journal of the Italian Association of Biomedical Physics (AIFB)* **24**, 129 (2008).
8. Davis, T., Gao, D., Gureyev, T., Stevenson, A. & Wilkins, S. Phase-contrast imaging of weakly absorbing materials using hard X-rays. *Nature* **373**, 595–598 (1995).
9. Tang, R. *et al.* Microbubble-based synchrotron radiation phase contrast imaging: basic study and angiography applications. *Physics in Medicine and Biology* **56**, 3503 (2011).
10. Xi, Y., Tang, R., Wang, Y. & Zhao, J. Microbubbles as contrast agent for in-line x-ray phase-contrast imaging. *Applied Physics Letters* **99**, 011101–011103 (2011).
11. Tang, R., Chai, W.-M., Yang, G.-Y., Xie, H. & Chen, K.-M. X-ray Phase Contrast Imaging of Cell Isolation with Super-Paramagnetic Microbeads. *PLoS one* **7**, e45597 (2012).
12. Tang, R. *et al.* Anti-VEGFR2-conjugated PLGA microspheres as an x-ray phase contrast agent for assessing the VEGFR2 expression. *Physics in Medicine and Biology* **57**, 3051 (2012).
13. Wilkins, S., Gureyev, T., Gao, D., Pogany, A. & Stevenson, A. Phase-contrast imaging using polychromatic hard X-rays. *Nature* **384**, 335–338 (1996).
14. Tang, L., Li, G., Sun, Y.-S., Li, J. & Zhang, X.-P. Synchrotron-radiation phase-contrast imaging of human stomach and gastric cancer: in vitro studies. *Journal of Synchrotron Radiation* **19**, 319–322 (2012).

## Acknowledgments

This work was supported by the Nation Basic Research Program of China (973 Program 2010CB834305) and Natural Science Foundation of China, Grant no. 81271740. We thank Honglan Xie and Yanan Fu for technical assistance.

## Author contributions

R.T. designed and performed experiments, analysed data and wrote the paper; W.X.L. and W.H. performed experiments; F.Y. and W.M.C. analysed data; G.Y.Y. and K.M.C. designed experiments and analysed data.

## Additional information

Supplementary information accompanies this paper at <http://www.nature.com/scientificreports>

**Competing financial interests:** The authors declare no competing financial interests.

**How to cite this article:** Tang, R. *et al.* CO<sub>2</sub>-based in-line phase contrast imaging of small intestine in mice. *Sci. Rep.* **3**, 2313; DOI:10.1038/srep02313 (2013).



This work is licensed under a Creative Commons Attribution-NonCommercial-NoDerivs 3.0 Unported license. To view a copy of this license, visit <http://creativecommons.org/licenses/by-nc-nd/3.0>